



**HAL**  
open science

# Interfacial adhesion in glass-fiber thermoplastic composites processed from acrylic reactive systems, a multi-scale experimental analysis

Q. Charlier, F. Lortie, J.-F. Gérard

► **To cite this version:**

Q. Charlier, F. Lortie, J.-F. Gérard. Interfacial adhesion in glass-fiber thermoplastic composites processed from acrylic reactive systems, a multi-scale experimental analysis. *International Journal of Adhesion and Adhesives*, 2020, 98, pp.102536 -. 10.1016/j.ijadhadh.2019.102536 . hal-03488574

**HAL Id: hal-03488574**

**<https://hal.science/hal-03488574>**

Submitted on 21 Dec 2021

**HAL** is a multi-disciplinary open access archive for the deposit and dissemination of scientific research documents, whether they are published or not. The documents may come from teaching and research institutions in France or abroad, or from public or private research centers.

L'archive ouverte pluridisciplinaire **HAL**, est destinée au dépôt et à la diffusion de documents scientifiques de niveau recherche, publiés ou non, émanant des établissements d'enseignement et de recherche français ou étrangers, des laboratoires publics ou privés.



Distributed under a Creative Commons Attribution - NonCommercial 4.0 International License

# Interfacial adhesion in glass-fiber thermoplastic composites processed from acrylic reactive systems, a multi-scale experimental analysis

Q. Charlier, F. Lortie and J.-F. Gérard

Université de Lyon, INSA Lyon, Ingénierie des Matériaux Polymères, UMR CNRS 5223,

F-69621 Villeurbanne, France ([frederic.lortie@insa-lyon.fr](mailto:frederic.lortie@insa-lyon.fr))

## Abstract

Interfacial adhesion in poly (methyl methacrylate) (PMMA)/glass fiber (GF) composites which are processed by in-situ polymerization of an acrylic reactive mixture, has been studied at both micro- and macro-scales. On one hand model systems were evaluated at microscale using the microbond test. On the other the 15° off-axis tensile test was used to assess the fiber/matrix interfacial adhesion at macroscale in real-sized thermoplastic (TP) composite parts. For each test, reference epoxy/GF samples were characterized alongside PMMA/GF composites. Results demonstrate that the fiber/matrix interfacial strength in PMMA/GF reaches 60% and 75% of the epoxy reference value at micro and macroscale, respectively. It proves the consistency of analyses at both scales. Thus, a micromechanical analysis relying on the microbond test appears as a reliable tool to estimate the fiber/matrix interfacial bond strength which is experienced in real-sized parts. Overall results also highlight the interest of manufacturing GF/PMMA composites through a reactive process to yield parts exhibiting strong interfacial properties. It may be promising for the development of thermoplastic solutions for structural composite applications.

## Keywords

resin-based composites, micro-shear, macro-shear, interfaces

## 1. Introduction

Nowadays, fiber-reinforced composites are widely used in various industrial sectors such as aerospace, automotive, public utility, sports and leisure. Historically, composite structures have been mainly designed using thermosetting polymer systems (TS). It is generally assumed that TS composites display better thermomechanical, chemical and creep resistance than thermoplastic ones (TP). On the other hand, TP composites exhibit advantages in terms of thermoformability, recyclability, and impact resistance especially when semi-crystalline. Nowadays, new environmental issues and in particular a growing need for recyclability motivate efforts to develop TP solutions. TP composites are commonly manufactured using non-reactive processes such as hot-pressing of pre-impregnated reinforcing plies [1]. Nevertheless, TP polymers usually exhibit a high viscosity at molten state which could limit fiber impregnation and interplies adhesion and consequently may alter final part mechanical performances.

Thus, efforts are paid to develop more reliable and cost-effective processing strategies for these materials. In this framework, reactive processes like resin transfer molding (RTM) or infusion constitute an appealing approach since they are based on a low-pressure injection of reactive precursors into a mold containing a dry preform. Such processes are usually involved in TS composite manufacturing but can be extended to TP composites provided that the polymer matrix can be obtained from low viscosity monomers ( $\leq 1$  Pa.s) [2]. In particular, recent works mention the use of polyamide-based [3] or polybutylene

terephthalate (PBT)-based [4-5] solutions to manufacture thermoplastic composites from low-viscosity precursors. If compared with standard TP processing methods, RTM or infusion are expected to yield composites with better interfacial adhesion. Indeed, since the viscosity of the impregnating resin is initially very low, one can expect a better intimate contact between matrix and reinforcing fibers, i.e. a better interfacial adhesion. Poly(methyl methacrylate) (PMMA) is a possible candidate for such a processing strategy since it can be obtained by radical polymerization of methyl methacrylate (MMA) using a thermal initiator [6, 7]. The radical polymerization of acrylic systems can take place at moderate temperatures and the processing cycle can also be adjusted by a careful choice of catalysts and inhibitors.

Interfacial adhesion between polymer matrix and reinforcing fiber strongly conditions final part performances and so can be measured to assess the potential of a new system [8, 9]. In our case, the state of the art on fiber-reinforced PMMA composites is actually quite poor whatever the processing method. The few publications identified in the literature are either focused on the study of similar PMMA/glass fiber (GF) systems but do not discuss interfacial issues [10], or dedicated to the study of interfacial properties in acrylic based-systems which quite differ from ours (thermosetting dental resins) [11]. Vallittu published a very interesting paper on the characterization of PMMA/GF composites which have been also obtained by in-situ polymerization of an acrylic resin onto glass fibers [12]. But the author chose a particular testing method which is not commonly used to assess the quality of the fiber/matrix bond. For its part Beguinél used low viscosity acrylic latices to manufacture PMMA/GF composites but even if her objectives were very close to ours, the involved acrylic systems stay unreactive [13]. The state of the art regarding interfacial properties in glass/thermoplastic composites manufactured from low-viscosity precursor is also quite

poor. Among the few reported works, Mäder used the pull-out test to investigate on PBT/GF interfaces [5]. More precisely, interfacial properties have been assessed according to the glass sizing nature (considering different chemistries and various surface roughnesses). However, the study is more focused on the sizing than on the thermoplastic matrix itself. In this context, the aim of our work is to evaluate the interfacial bond strength between PMMA and glass fiber in the case of an interface generated by radical polymerization of a low-viscosity acrylic resin onto the fiber. It is well known that interfacial properties result from a combination of several mechanisms occurring at various scales. Thus, our strategy is to focus on interfacial properties at both micro- and macro- scales to dissociate fiber/matrix interactions from process-induced effects. To reach such a goal, microdroplets have been prepared using optimized polymerization conditions (formulation, temperature). The microbond test has been carried out on PMMA/GF and epoxy/GF specimens to evaluate the interfacial adhesion at microscale. Then, unidirectional (UD) composites have been prepared and characterized using the 15° off-axis tensile test. All collected results have been confronted to assess the quality of the fiber/matrix bond.

## 2. Characterization methods for the assessment of fiber/matrix interfacial properties

Many characterization methods are available to assess the quality of the fiber matrix/bond at different scales [14]. In this work, two tests have been selected based on several criteria: compatibility with acrylic reactive systems, repeatability, relevancy with the scale of study, ease of implementation, amount of related literature.

### 2.1. Microbond test

Miller proposed this test as an alternative to the pull-out test [15]. A droplet of polymer precursor is deposited onto a single stretched filament. After curing, the microcomposite specimen is fixed onto a paper support, mounted between clamps in a tensile machine, and finally debonded (Figure 1a)).

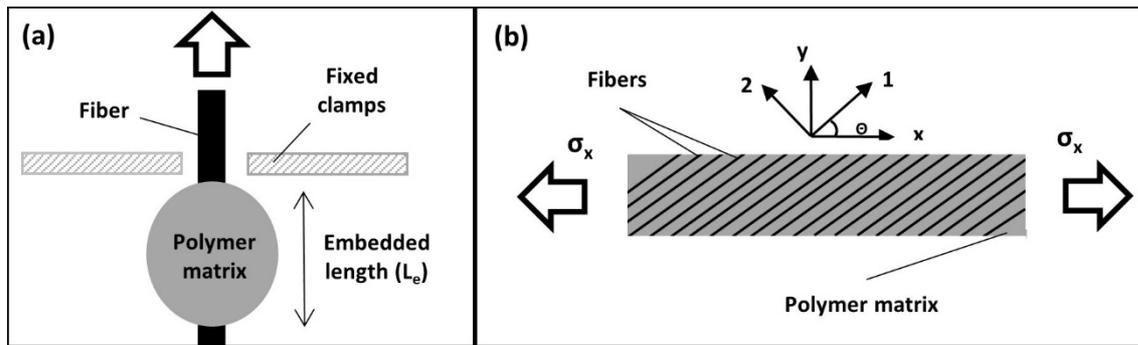


Figure 1: The microbond test (a), and the off-axis tensile test (b).

To estimate the interfacial adhesion, several stress-based and energy-based models are described in the literature depending on the sample failure mode [14 ,16]. Models compute physical parameters of both matrix and fiber as well as sample and device geometries. The most famous one is built on a stress-based approach assuming a plastic behaviour of the matrix when debonding occurs, i.e. the shear stress is considered constant along the embedded fiber. The average interfacial shear strength (IFSS),  $\tau$ , is given by:

$$\tau = \frac{F_d}{\pi d_f l_e} \quad (1)$$

where  $l_e$  is the embedded length,  $F_d$  is the debonding force, and  $d_f$  is the fiber diameter. This approach requires an adhesive failure between fiber and matrix to be valid.  $\tau$  is a conventional parameter which is related to the different phenomena contributing to the debonding (fiber/matrix bond, friction,...). Therefore, it is an apparent interfacial shear strength and it must not be confounded with the adhesion strength relative to the

fiber/matrix bond. Moreover, the stress field that is generated by the debonding process is in fact not constant all along the embedded fiber as suggested by Equation (1) [17]. Nevertheless, the IFSS calculation based on the microbond test has several advantages: i) it is quite easy to set-up (considering it is a micro-scale procedure), ii) results are highly reproducible from one experimenter to another, iii) the IFSS calculation is a straightforward and popular method to quantify adhesion. The last statement is especially true if compared to other micromechanical tests such as fragmentation. In particular, fragmentation is a well-recognized procedure to evaluate interfacial adhesion in fiber/matrix systems. However, estimating interfacial adhesion using the latter is not as straightforward as it is for microbond even when using the simplest models. Thus, it is very difficult to find data reduction techniques which can efficiently assess interfacial adhesion in polymer/fiber systems presenting different types of matrices [18]. It is the main reason why the microbond procedure was chosen rather than other microscale testing methods. It is also recognized by others as a straightforward and reliable method adapted to the physicochemical analysis of fiber/matrix interactions [19].

## 2.2. Off-axis tensile test

When a unidirectional (UD) fiber reinforced composite is shear-loaded, strains are concentrated near interfacial zones [20]. Thus, interfacial properties in UD composites, i.e. the fiber/matrix adhesion, are shear-related. The associated parameters are the shear modulus,  $G_{12}$ , and the shear strength,  $\tau_{12m}$ .

The stress state in UD composites strongly depends on the stretching direction. Chamis found out that for a critical loading angle,  $\vartheta_c$ , the normalized shear strain,  $\varepsilon_{12}$ , is 7 to 8 times greater than both longitudinal and transverse strains [20]. In fact, the value of  $\vartheta_c$  results

from the difference in stiffness between matrix and fiber, i.e. it depends on the nature of the component ( $\vartheta_c = 15^\circ$  for glass/epoxy composites). As it can lead to an almost-pure shear-induced stress field, the off-axis tensile test appears as an interesting strategy for assessing and enhancing the interface response (Figure 1b). Using a conventional rotation matrix, the shear stress,  $\tau_{12}$ , can be expressed as a function of the applied stress in the loading direction,  $\sigma_{xx}$ , and the deviation angle between the loading and the fiber direction,  $\vartheta$ :

$$\tau_{12} = \frac{\sigma_{xx} \sin 2\vartheta}{2} \quad (2)$$

Equally,  $\varepsilon_{12}$  can be expressed from the elementary strains in the loading direction (x,y),  $\varepsilon_{xx}$ ,  $\varepsilon_{yy}$ , and  $\varepsilon_{xy}$ :

$$\varepsilon_{12} = (\varepsilon_{yy} - \varepsilon_{xx}) \sin 2\vartheta + \varepsilon_{xy} \cos 2\vartheta \quad (3)$$

where  $\varepsilon_{12}$  is the shear strain in the fiber direction, and  $\vartheta$  is the deviation angle between the tensile axis and the fiber direction. The shear modulus,  $G_{12}$ , and the ultimate shear strength,  $\tau_{12m}$ , can finally be deduced from the analysis of the strain/stress trace  $\varepsilon_{12}$  versus  $\tau_{12}$ ,  $G_{12}$  being the half of the slope at low strains:

$$G_{12} = \frac{\tau_{12}}{2\varepsilon_{12}} \quad (4)$$

While the off-axis tensile test is not the most common method to assess the interfacial properties of a composite, it is for us the most relevant one. Indeed, three and four-points bending tests are known to generate complex stress states constituted of tension, compression, and shear stresses even with optimized thickness-to-length ratios. The  $45^\circ$  tensile test can also lead to the assessment of shear properties with a correct analysis but it does not generally lead to a shear-related failure. The transverse tensile test is irrelevant as the associated modulus mostly depends on matrix properties. The  $10\text{-}15^\circ$  off-axis tensile

test was not so common 30 years ago due to the complexity of setting up reliable gauges and also because of the large quantity of collected data to be analyzed. But considering current computing capacities and new technics such as digital image correlation, this test should regain in interest.

### 3. Experimental section

#### 3.1. Materials

Acrylic matrices are obtained by radical polymerisation of an acrylic resin supplied by Arkema (Paris, France). The resin is composed of atactic PMMA ( $M_w=100,000 \text{ g}\cdot\text{mol}^{-1}$ ) dissolved in a blend of acrylic monomers (mainly MMA) by mechanical stirring. The PMMA content lies between 20 and 25wt.%. It is adjusted to reach the appropriate viscosity (in that case 0.3Pa.s). Polymerization is triggered at room temperature using an initiating system composed of a thermal initiator, benzoyl peroxide (BPO) (1 per hundred resin (phr) of commercial product), and a tertiary amine catalyst, dihydroxyethyl-p-toluidine (DHEPT) (in equimolar proportions with BPO) supplied by Sigma Aldrich (Saint-Louis, MO, USA) . A thermosetting (TS) DGEBA-based epoxy system currently used for composite applications is used as reference. When the epoxy system is cured following the recommendation of the supplier, both matrices present similar mechanical properties at 25°C. The acrylic matrix has a 2.5GPa E-modulus and a 55MPa strength at break. The epoxy reference has a 2.8GPa E-modulus and a 77MPa strength at break. Densities are  $1.18\text{g}/\text{cm}^3$  for PMMA and  $1.16\text{g}/\text{cm}^3$  for epoxy. The glass transition temperature ( $T_g$ ) of cured PMMA is around 110°C whereas the epoxy network shows two  $T_g$  (70°C and 110°C). ). Regarding many aspects (cured and uncured material properties, processability, and relevancy regarding our project), this epoxy system is one of the best to discuss the interest of our acrylic system. This is why we chose it

as reference even if its exact composition cannot be disclosed owing to confidentiality issues.

Advantex® E-CR glass reinforcing fibers are supplied by 3B-Fiberglass (Herve, Belgium) (density=2.62g/cm<sup>3</sup>, tex=1200kg/m, E=81-83GPa,  $d_f = 17.9 \pm 1.2 \mu\text{m}$ ). According to the supplier, the fiber sizing is compatible with both epoxy and acrylic systems. Unfortunately, neither the exact reactive chemical groups nor the nature of the film former are known. UD plies are cut out from a fabric roll provided by Chomarat (Le Cheylard, France) (weft proportion  $\approx 3\%$ , width=11cm).

### 3.2. Preparation and characterization of microdroplets

Single glass filaments are pre-stressed and fixed onto a metallic frame. Resin droplets are deposited onto the fibers with a copper thread ( $\varphi=100\mu\text{m}$ ) and then cured 1h at 80°C and post-cured 2h at 160°C. Acrylic and epoxy droplets were polymerized according to the same curing conditions. Then, 40 to 50 fibers are cut and stuck onto a paper support for each type of resin. The embedded length,  $l_e$ , is determined by OM. At this point, some samples are discarded when observing asymmetrical droplets, too high embedded lengths, or droplet-free fibers. Finally, droplets are debonded between two razor blades at 0.1mm/min at room temperature using a MTS 2/M tensile testing machine (MTS System, Turin, Italy) equipped with a 10N sensor. To monitor the test, a SVCam-ECO655 camera (SVS Vistek, Seefeld, Germany) is used with a macrozoom objective to record the debonding process. 24 acrylic droplets and 24 epoxy droplets have been tested. All specimens are observed after testing by OM (BF, RL, x500) to check that the failure mechanism is in agreement with the IFSS calculation. Reference epoxy-based microdroplets are prepared and tested in similar conditions. An additive was added in the acrylic resin to prevent the evaporation of acrylic

monomers while preparing droplets (paraffin wax, 0.7phr, provided by Sasol, Hamburg, Germany). It is not possible to prepare acrylic droplets otherwise.

One can observe that high curing temperatures were chosen despite the fact that the system is able to polymerize at room temperature. In fact, the radical polymerization of such acrylic systems is highly exothermic. The produced heat allows the reaction to go on and triggers specific phenomena such as Trommsdorff's effect which are necessary to reach a full conversion at low temperature [6, 7, 21, 22]. In bulk conditions, i.e. for several grams of resin, the temperature can reach up to 80-110°C depending on initiating system content and nature [6, 10]. But processing microbond samples involves a very low amount of reactive mixture (about a tenth of milligram). It is very difficult to investigate on thermal aspects at this scale. Our assumptions are that the reaction does not autoaccelerate as it is supposed to do in bulk conditions and so the reaction extent is not as high. To a lesser extent, we think that epoxy systems are also affected by this change of scale. We noticed that epoxy droplets are not fully cured when using the curing conditions recommended by the supplier. Thus, a high postcure temperature was chosen to make sure that matrix droplets are fully cured.

### 3.3. Preparation and characterization of off-axis tensile specimens

PMMA-based composites are obtained by infusion onto a glass plate at room temperature (3 plies of 30x11cm<sup>2</sup>, 0.1 bar, 2 to 3 minutes). After vitrification, UD parts are released to be post-cured for 1h at 100°C. Reference epoxy composites are processed by hot-compression using a Satim hot-press (Satim group, Le Raincy, France) (10 minutes, 110°C, 5 bars). UD plies are manually impregnated, stacked, and placed between two Teflon non-adhesive sheets.

The quality of acrylic and epoxy composites is controlled by density and fiber content measurements as well as SEM observations. Density and fiber content measurements are performed for each composite on 4 samples of 30x30mm<sup>2</sup>. Samples are cut using a “Charly 4U” milling machine (Charlyrobot, Cruseilles, France). Cutting conditions are 8,000rpm rotation speed and 4mm/s advance speed using a 3mm-diameter milling tool for plastic machining. Density measurements are performed by hydrostatic weighing using a density kit from Mettler Toledo for precision balances (Columbus, Ohio, United States). The density,  $\rho$ , is calculated from the weight of dried sample in air,  $m_d$ , the weight of sample immersed in water,  $\mu$ , and the weight of humid sample in air,  $m_h$ , according to:

$$\rho = \frac{m_d \rho_w}{m_h - \mu} \quad (5)$$

where  $\rho_w$  is the water density at the temperature of experiment.

Fiber weight contents are determined by pyrolysis. Composite samples are pyrolyzed at 650°C for several hours. Fiber content,  $x_f$ , is assessed by weighing crucibles before and after the thermal treatment according to:

$$x_f = \frac{m_r - \left( \frac{m_s - m_r}{1 - x_{rm}} \right)}{m_s} \quad (6)$$

where  $m_s$  is the initial mass of the sample,  $m_r$  is the remaining mass after pyrolysis, and  $x_{rm}$  is the matrix residual content at 650°C (8.2wt.% for epoxy, 0.2wt.% for acrylic). Assuming that composites are parallelepiped samples only composed of fiber, matrix, and air, the porosity content, or air volume fraction,  $\varphi_a$ , can be estimated from  $\rho$  and  $x_f$  according to:

$$\varphi_a = 1 - \left( x_f \frac{\rho}{\rho_f} + (1 - x_f) \frac{\rho}{\rho_m} \right) \quad (7)$$

where  $\rho_f$  and  $\rho_m$  are the densities of the fiber and the matrix, respectively. Based on the same assumptions, the fiber volume content,  $\varphi_f$ , can be estimated from  $\rho_m$ ,  $\rho_f$ ,  $x_f$ , and  $\varphi_a$  according to:

$$\varphi_f = 1 - \varphi_a - (1 - \varphi_a) \left[ 1 - \frac{\frac{x_f}{\rho_f}}{\frac{1-x_f}{\rho_m} + \frac{x_f}{\rho_f}} \right] \quad (8)$$

To observe the composites, specimens are polished perpendicularly to warp direction using a Presi Minitech 233 device (Presi, Eybens, France). 3 diamond-based polishing discs of grain size 600, 2400, and 4000 are successively used for polishing. Initial rotation speed is set to 200rpm. Speed is slowed down to 150 and ultimately 100rpm when increasing the polishing grade. The procedure takes 10 to 15 minutes to obtain a correct polishing. SEM pictures are taken with a Phillips XL20 microscope (secondary electron detector, tension of acceleration of 10kV , spotsize 5, up to x500) (Phillips, Amsterdam, Netherlands). Samples are previously metallized using a Bal-Tec SCD005 sputter coater to deposit a 10nm gold layer (Scotia, NY, United States).

Off-axis specimens are cut out with a deviation of 15° from warp direction using the same machining conditions than the ones applied to density samples. Epoxy/glass end-tabs are bonded using a Loctite 3425 bi-component adhesive and a speckle pattern is painted on the tested lengths. Off-axis samples are then tested using a MTS 2/M tensile testing machine equipped with a 10kN sensor operating at 0.5mm/min. The shear stress,  $\tau_{12}$  (fiber direction), is calculated from the measured  $\sigma_{xx}$  (loading direction) (Equation (2)). Tensile tests are recorded using a SVCam-ECO655 camera equipped with a telecentric objective. The evolution of the strain field with time is assessed by digital image correlation using the software UFreckles developed by LAMCOS Laboratory (UMR 5259, University of Lyon,

France). The software calculates the average changes in  $\epsilon_{xx}$ ,  $\epsilon_{yy}$ , and  $\epsilon_{xy}$  (loading direction) from the recorded pictures on an approximate surface of  $40 \times 10 \text{ mm}^2$ . Then, the evolution of  $\epsilon_{12}$  (fiber direction) with time is calculated using Equation (3). Finally, the  $\tau_{12}$  vs  $\epsilon_{12}$  traces are established and the shear modulus,  $G_{12}$ , is determined by settling a linear regression in the elastic domain ( $\epsilon_{12}$ ,  $1\text{E}^{-4}$  to  $1\text{E}^{-3}$ ).  $G_{12}$  and  $\tau_{12m}$  are averaged on 4 samples. Fracture surfaces of failed off-axis specimens are observed by SEM in the same conditions than described earlier though samples are not polished.

One can notice that different processing methods were used to prepare acrylic and epoxy UD specimens. However, this study focuses on assessing the fiber/matrix interfacial properties by relying on characterization methods which selectively probe interfaces. To our opinion, the processing method is expected to have little influence on fiber/matrix interfacial properties as long as fiber and porosity contents are the same and curing conditions are respected. Epoxy specimens were prepared following the recommendations of the supplier. Several processing methods were tested beforehand to prepare acrylic composites. The best specimens were obtained using an infusion process which explains why two different processing methods are used.

## 4. Results and discussion

### 4.1. Microbond test

Typical failures of microbond samples can be observed in Figure 2. Only one adhesive failure mode was observed. The presence of a residual meniscus attests of a failure initiation according to a mode I followed by a propagation according to a mode II. Matrices were also damaged by the fixed clamps during debonding which suggests that a part of the debonding

force,  $F_d$ , is used to plasticize and break the matrix. The recorded force/displacement curves are consistent with reported data [15] (Figure 3). After debonding, the sensor is still recording constant frictional forces of close values for all droplets. It confirms that the apparent IFSS calculated from Equation (1) results from more contributions than the sole fiber/matrix adhesion.

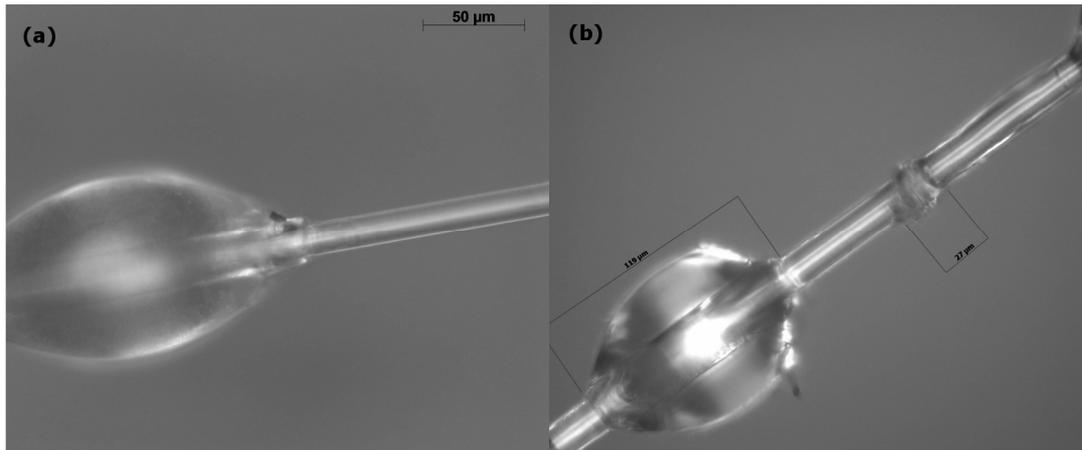


Figure 2: Adhesive failure of a PMMA/GF (a) and of an epoxy/GF (b) droplets characterized using the microbond test (OM, BF-RL, x500).

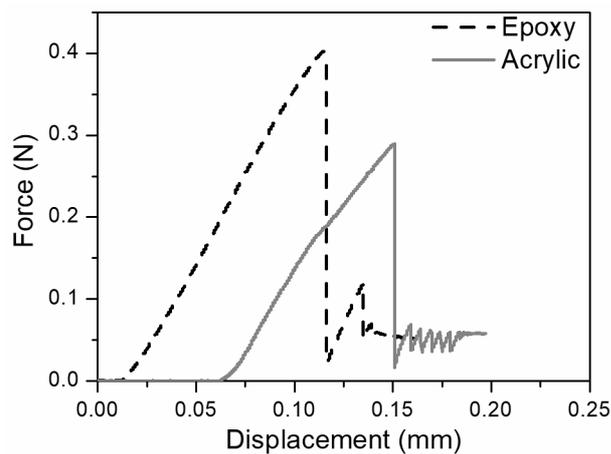


Figure 3: Typical force/displacement traces of the debonding process for acrylic and epoxy droplets (room temperature, 0.1mm/min).

Debonded forces vs embedded lengths for acrylic and epoxy droplets are shown in Figure 4. On the 24 tested samples, 20 acrylic droplets have been debonded and 4 fibers have broken before debonding. On the other hand, 14 epoxy droplets have been debonded and 10 fibers have broken before debonding. Only the debonded droplets were considered in Figure 4 and for the IFSS calculation. Epoxy droplets present a better interfacial adhesion than the acrylic ones, i.e. higher debonding forces are observed for shorter lengths (Figure 4). Interfacial adhesion is higher in epoxy/GF than in PMMA/GF systems (43 for 26 MPa, Table 1).

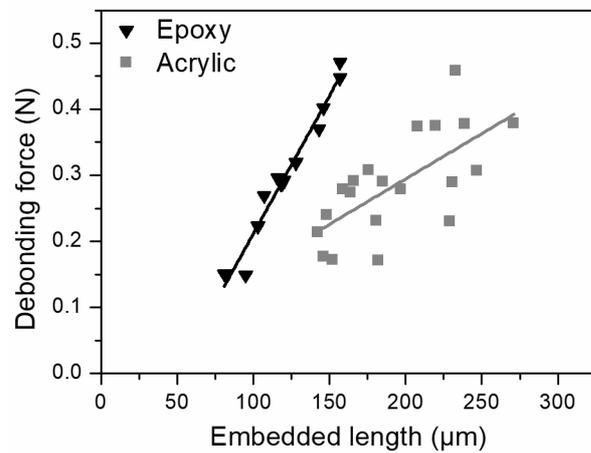


Figure 4: Debonding forces versus embedded lengths for epoxy and acrylic microdroplets.

Testing method	15° off-axis		Microbond
Adhesion parameter	$G_{12}$	$\tau_{12m}$	M-IFSS
	GPa	MPa	MPa
Acrylic	$2.8 \pm 0.1$	$29 \pm 1$	$26 \pm 5$
Epoxy	$3.0 \pm 0.1$	$38 \pm 1$	$43 \pm 7$

Table 1: Adhesion parameters determined by the microbond and the off-axis tensile tests.

The quasi-linear variation of  $F_d$  with  $l_e$  is consistent with Equation (1). However a large dispersion of data is also evidenced: it can be explained by the fact that additional

parameters which are not displayed in Equation (1) also influence results [14, 19]. For example, the fiber free length (distance between the droplet and the attachment point) as well as the distance between the blades are known to influence the debonding force and sometimes even the failure mode. Unfortunately, these parameters are different for each tested microdroplet considering that the procedure is not automated. Consequently, a good reproducibility of the testing conditions is difficult to achieve.

One can notice that the number of fiber breaks is quite important for epoxy droplets. It is due to a problem of fiber free length. To ensure that the fiber does not break during the tensile test, its free length was kept as short as possible. However, it is very difficult to minimize it when preparing microdroplets manually. Sometimes the free length could be up to a few millimetres. If we look at the average fiber break force and the average debonded force, values are quite similar for both systems (acrylic droplets:  $F_{break}=0.279\text{N}$  and  $F_d=0.286\text{N}$ ; epoxy droplets:  $F_{break}=0.355\text{N}$  and  $F_d=0.297\text{N}$ ). More fiber breaks were observed with epoxy droplets because the average failure force was higher than for acrylic droplets. Anyway, the distribution  $F_d$  vs  $L_e$  is still looking good for epoxy/GF so we do not think our results were too much altered by this phenomenon. But due to the high number of breaks, we keep in mind that the epoxy/GF IFSS may be slightly underestimated.

The spread of data is also slightly broader for acrylic droplets compared to epoxy ones. In our opinion, two phenomena could explain this discrepancy. PMMA matrices are obtained through a chain-wise polymerization mechanism which usually leads to inhomogeneous materials (large mass distributions) while epoxies polymerize through a step-wise mechanism which yields more homogeneous matrices. Moreover, as explained in the experimental section, we have some doubts about how goes the polymerization of these

acrylic systems at microscale. In particular, we are not sure of the reproducibility of the polymerization reaction from one droplet to another. Unfortunately, investigations could not be pushed further.

Based on literature data, an IFSS value of 50 to 90 MPa is expected for epoxy or vinyl ester/GF microcomposites which is much higher than our results [15, 19, 23]. The IFSS measured on our acrylic droplets is closer to values obtained with other TP/GF systems based on PA6 (20-50 MPa [24, 25]), PMMA (10-20 MPa [13]), or PP (5-25 MPa [26]). Unfortunately, the latter were not in-situ polymerized onto glass fibers and it would have been more relevant to compare performances of TP/GF systems obtained through a reactive strategy. But the related literature is scarce and we were not able to find such kind of studies. However, Beguinél thesis work is an interesting reference to discuss the benefits of a reactive strategy for the improvement of PMMA/GF interfacial adhesion [13]. The author prepared PMMA/GF microcomposites by deposition of a non-reactive acrylic latex onto glass fibers. In both cases, a good impregnation is expected considering the low viscosity of acrylic precursors. Nevertheless, no chemistry is involved in latex consolidation, i.e. the adhesion mainly originates from physical interactions. In our case, chemical bonding can be expected due to reactions between activated radicals and sizing molecules during polymerization. Comparing our mean IFSS value (26MPa) to Beguinél one (20MPa), it seems that the reactive strategy brings an additional contribution of the order of 15% to the fiber/matrix adhesion. Another interesting reference is the study of McDonough who performed debonding tests on GF/acrylic composites prepared from acrylic dental resins [11]. The IFSS reaches slightly higher values in these microcomposites compared to ours (from 15 to 34MPa depending on the silane agent and water exposure). Nevertheless, acrylic dental resins are known to yield cross-linked materials. They may not be the best

systems to assess the performances of our PMMA/GF interfaces despite the close chemical nature and processing strategy. Mäder's study can also be mentioned as the author worked on PBT/GF microcomposites prepared from a reactive low-viscosity resin and tested using pull-out [5]. Even if the testing geometry slightly differs from microbond, the same hypotheses are used to estimate interfacial adhesion. Thus, related values constitute a good comparison point. Unsized PBT/GF microcomposites show an IFSS of 16MPa. Sized PBT/GF microcomposites show IFSS values from 20 to 41MPa depending on sizing formulation. It is slightly higher than the ones of our PMMA/GF droplets. The large range of IFSS obtained by Mäder when changing the sizing also suggests there is room for improvement for PMMA/GF systems. However, as the study is focused on the effect of sizing on interfacial adhesion, the properties of the resin/matrix are not so much discussed. The author only indicates that the non-homogenous nature of the polymer matrix limits the potential of further improvement of fiber/matrix interfacial adhesion.

#### 4.2. Off-axis tensile test

For two main reasons, it is important to check the quality of the manufactured composites before performing any off-axis tensile test. First, a high porosity content can badly affect mechanical properties. More importantly, it can also change the failure mechanism. A too high porosity content will end up in a failure related to the distribution of porosity instead of a fiber/matrix interfacial failure. Secondly, the fiber content greatly affects mechanical properties [27]. Thus, acrylic and epoxy composites must show close fiber contents for the study to be relevant. Close values of density,  $\rho$ , and fiber weight content,  $x_f$ , were found for both studied systems (Table 2). Moreover, the porosity volume content,  $\phi_a$  is 2.7 vol.% for acrylic and 0 vol.% for epoxy which is considered as satisfying to conduct the off-axis tensile

procedure and to get an interfacial related failure. SEM observations have confirmed that porosity is very low in both composites. Pictures of acrylic and epoxy cross-sections are shown in Figure 5. More specifically, epoxy composites show a little porosity inside some of the tows but no porosity between the tows (Figure 5). On the opposite, acrylic composites show no porosity inside the tows but sometimes the resin does not fully fill the space between tows which can lead to surface defects (in particular at the edges of the plate). It results in additional uncertainties in our density and porosity calculation as we considered a full parallelepiped. This can explain the differences in the calculated porosities as well.

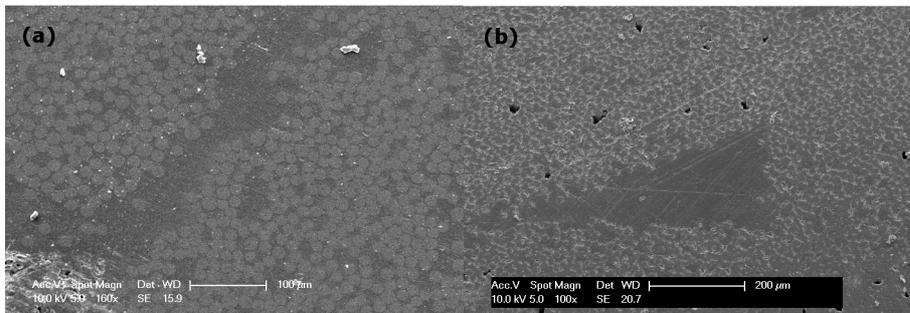


Figure 5: SEM cross-sections of an acrylic (a) and an epoxy (b) composites characterized using the off-axis tensile test (SE, x160).

Parameter	$\rho$ g/cm <sup>3</sup>	$x_f$ wt. %	$\phi_f$ v. %	$\phi_a$ v. %
Acrylic	2.04	79.3	61.2	2.7
Epoxy	2.05	77.0	59.8	0.0

Table 2: Density ( $\rho$ ), fiber weight content ( $x_f$ ), fiber volume content ( $\phi_f$ ) and porosity volume content ( $\phi_a$ ) measured on acrylic and epoxy composites (subsequently characterized using the off-axis tensile test). Values were calculated from Equation (5) to (8).

Typical in-axis strain/stress curves are shown in Figure 6. Shear strains at break of 1 to 2% were generally measured. Shear strains,  $\epsilon_{12}$ , were found to be 5 to 7.5 times greater than

the longitudinal and transverse strains,  $\epsilon_{11}$  and  $\epsilon_{22}$ , which is consistent with Chamis's work [20]. Moreover, all fracture profiles observed by SEM show interfacial failures (Figure 7). These observations validate the conditions of almost-pure shear load and interfacial failure which were the main reason for selecting this test.

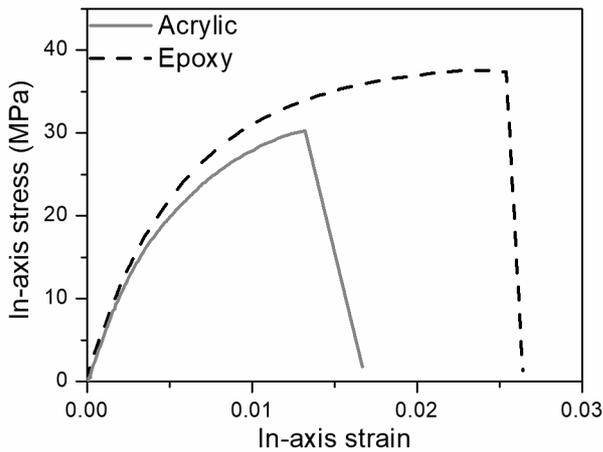


Figure 6: Typical in-axis strain/stress curve of the 15° off-axis tensile test performed on UD acrylic and epoxy composites (room temperature, 0.5mm/min).

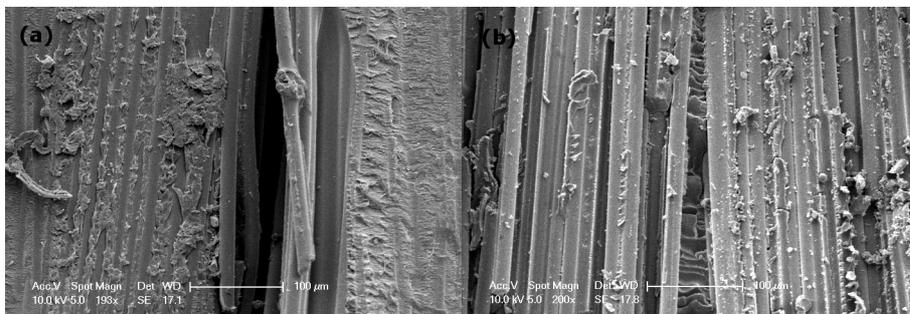


Figure 7: SEM pictures of shear failures in acrylic (a) and epoxy (b) composites characterized by the off-axis tensile test (SE, x200).

Concerning shear properties, shear moduli,  $G_{12}$ , of acrylic and epoxy composites are very close (2.8 and 3.0 GPa, respectively) (Table 1). On the other hand, the ultimate shear strength,  $\tau_{12m}$ , is higher for epoxy/GF composites (29 and 38 MPa). The different tendencies given by  $G_{12}$  and  $\tau_{12m}$  are consistent with several studies which have shown that  $G_{12}$  also

depends on matrix properties and fiber fraction [27, 28]. Thus, the sole comparison of  $G_{12}$  values to evaluate interfacial properties does not appear as sufficient [28]. Such a study could be relevant for comparing composites made of the same matrix and fiber fraction but different fiber sizings. In our case,  $\tau_{12m}$  is the most relevant parameter to discuss the fiber/matrix adhesion at macroscale.

Only a few similar studies relying on the off-axis tensile test have been reported so far. Moreover, comparison with literature data is uneasy due to the differences in experimental parameters and conditions. In particular, the influence of the fiber content on mechanical properties is very bothering [27]. Several other phenomena have also been identified as important sources of uncertainty such as the use of inappropriate tabs [29] or fiber misalignment during composite preparation [20]. Generally, epoxy/GF UD composites exhibit  $\tau_{12m}$  values lying in between 40 and 70 MPa [20, 27, 29]. As for the microbond analysis, our epoxy/GF reference shows lower properties than reported data. It may be explained by some experimental issues (see Microbond test result section). Another explanation could be that our system is already commercialized for a specific application which addresses other properties than fiber/matrix adhesion performances. Unfortunately, it seems that there is no reported study on TP/GF systems assessed using the 10-15° off-axis tensile test. The closest study identified in the literature was done by Vallittu on PMMA/GF composites obtained by in-situ polymerization of an acrylic resin onto glass fibers [12]. However, the author characterized the fiber/matrix adhesion using a testing method which induces a complex stress state (combining tension, compression and shear) and not a pure shear state as the off-axis tensile test provides. As a consequence, the measured strengths which are much higher than ours cannot be used as reference values.

### 4.3. Correlation of results obtained at different scales

One of the objectives of this study is also to compare data obtained both at microscale and macroscale to identify any correlation between them. The question is: is it possible to predict interfacial properties in composite parts by solely relying on micromechanical analyses (assuming that preparation step is optimized)? So far, very few similar approaches have been reported on epoxy/carbon fiber composites by Herrera-Franco and Drzal [9, 14] and on epoxy, PA6, and PP/carbon fiber composites by Mäder [24]. In particular, Mäder's work is very interesting as the author showed a strong correlation between micro and macro interfacial properties in epoxy/carbon composites for several fiber surface treatments [24]. However, different testing methods were used in these studies (single fiber fragmentation and pull-out tests at microscale, and bending and 45° tensile tests at macroscale). Moreover, none of these studies have considered glass fibers.

An absolute and a relative representation of IFSS and  $\tau_{12m}$  values associated to the acrylic/GF and the epoxy/GF systems are given in Figure 8. Results indicate that PMMA/GF interfacial strength reaches 60% of epoxy/GF properties as measured on microbond samples and 75% on UD composites (Figure 8b). This is a quite good result considering that this is the first characterization of the type using an acrylic reactive system, i.e. the acrylic resin has not been especially optimized so far for composite performances. It highlights the scientific interest of such thermoplastic solution to manufacture structural composites. However, further studies are needed to perform a full assessment of the mechanical properties of acrylic thermoplastic composites.

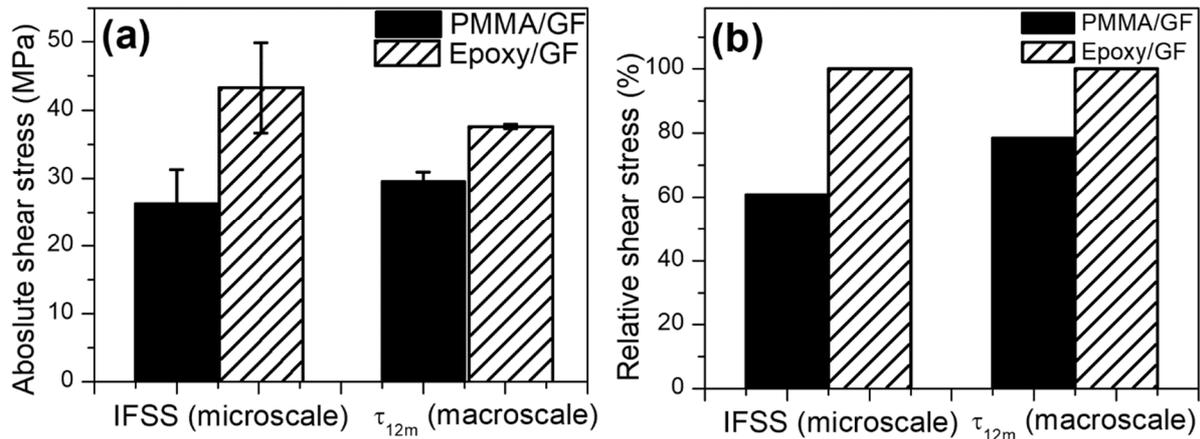


Figure 8: Multi-scale correlation of absolute (a) and relative (b) interfacial strengths in PMMA/GF and epoxy/GF composites. Relative values are weighted by the interfacial strength of the reference system.

It is also interesting to focus on raw strengths. As IFSS and  $\tau_{12m}$  share the same dimension, they can theoretically be directly compared. IFSS and  $\tau_{12m}$  values are very similar: 25MPa and 29MPa for PMMA/GF, and 43MPa and 38MPa for epoxy/GF, respectively (Figure 8a). Thus, the fiber/matrix strength does not seem to be affected by the change of scale in our case. Consequently, a micromechanical analysis relying on the microbond test appears as a reliable tool to estimate the fiber/matrix interfacial bond strength which is experienced in real-sized parts. Unfortunately, the lack of literature data on this subject does not allow us to extend such comparison. The study should be performed on other fiber sizings or fiber/matrix systems to confirm these results and to identify stronger correlations such as Mäder did [24].

One has also to keep in mind that this comparison must be done very carefully. Its aim is only to be used as a tool to estimate macroscale shear properties from micromechanics. It is true that IFSS and  $\tau_{12m}$  are both failure criteria characterizing the fiber/matrix interfacial strength at different scales. But they have been estimated assuming several hypotheses,

calculation methods, and experimental devices. Another critical point is that microcomposites highly differ from real-sized parts in terms of fiber volume content. In real-sized composites, fibers are more numerous and very close to one another. On the opposite, microdroplets (and microcomposites in general) are prepared on one filament. Consequently, the interphase conformation, the distribution of residual stresses, and the induced stress state under load are expected to be different.

## 5. Conclusion

The interfacial adhesion between fiber and matrix in PMMA/GF thermoplastic composites obtained by reactive processing has been investigated at micro and macro-scale. The microbond test has been used to evaluate the microscale interfacial adhesion in model composites. UD real-sized composites have also been prepared and tested through the 15° off-axis tensile method to probe interfaces at the macroscale. Both micro and macro-analyses show similar trends and respective data are consistent. Thus, a micromechanical analysis based on the microbond test appears as a reliable tool to predict the fiber/matrix interfacial bonding that could be experienced in real-sized parts, even if this analysis should be extended to other fiber/matrix systems to confirm the tendency observed in this study. PMMA/GF composites display a good interfacial adhesion close to those exhibited by standard epoxy/GF systems without any specific addition in the formulation of the acrylic resin to enhance composite performances (60% and 75% of the epoxy reference value at micro and macroscale, respectively). An extra contribution to the fiber/matrix adhesion seems to be brought by the use of a reactive strategy. Results are very encouraging for the development of thermoplastic composite manufacturing by reactive processing. Additional

studies are now required to assess the overall mechanical properties of these acrylic composites in order to verify their suitability for structural applications.

## Acknowledgements

The authors thank the FUI (Fond Unique Interministeriel) for financial funding.

## References

- [1] A.G. Gibson, J.A. Manson, Impregnation technology for thermoplastic matrix composites, *Composite Manufacturing*, 3 (1992) 223-233.
- [2] K. van Rijswijk, H.E.N. Bersee, Reactive processing of textile fiber-reinforced thermoplastic composites - An overview, *Composites, Part A*, 38 (2007) 666-681.
- [3] A. Luisier, P.E. Bourban, J.A.E. Manson, Reaction Injection Pultrusion of PA12 Composites: Process and Modelling, *Composites, Part A*, 34 (2003) 583-595.
- [4] H. Parton, J. Baets, P. Lipnik, B. Goderis, J. Devaux, I. Verpoest, Properties of poly(butylene terephthalate) polymerized from cyclic oligomers and its composites, *Polymer*, 46 (2005) 9871-9880.
- [5] E. Mäder, S.L. Gao, R. Plonka, J. Wang, Investigation on adhesion, interphases, and failure behaviour of cyclic butylene terephthalate (CBT®)/glass fiber composites, *Compos. Sci. Technol.*, 67 (2007) 3140-3150.
- [6] A. Zoller, D. Gimes, Y. Guillaneuf, Simulation of radical polymerization of methyl methacrylate at room temperature using a tertiary amine/BPO initiating system, *Polym. Chem.*, 6 (2015) 5719-5727.
- [7] Q. Charlier, J.C. Fontanier, F. Lortie, J.P. Pascault, J.F. Gerard, Rheokinetic study of acrylic reactive mixtures dedicated to fast processing of fiber-reinforced thermoplastic composites, *J. Appl. Polym. Sci.*, 136 (2019) 47391-47400.

- [8] I. Verpoest, M. Desaegeer, J. Ivens, M. Wevers, Interfaces in Polymer Matrix Composites From Micromechanical Tests to Macromechanical Properties, *Macromol. Symp.*, 98 (1993) 85-98.
- [9] L.T. Drzal, M. Madhukar, Fibre-matrix adhesion and its relationship to composite mechanical properties, *J. Mater. Sci.*, 28 (1993) 569-610.
- [10] D.S. Cousins, J. Howell, Y. Suzuki, J.R. Samaniuk, A.P. Stebner, J.R. Dorgan, Infusible acrylic thermoplastic resins: Tailoring of chemorheological properties, *J. Appl. Polym. Sci.*, 136 (2019) 48006-48021.
- [11] W.G. McDonough, J.M. Antonucci, J.P. Dunkers, Interfacial shear strengths of dental resin-glass fibers by the microbond test, *Dent. Mater.*, 17 (2001) 492-498.
- [12] P.K. Vallittu, Curing of a silane coupling agent and its effect on the transverse strength of autopolymerizing polymethylmethacrylate-glass fibre composite, *J. Oral Rehabil.*, 24 (1997) 124-130.
- [13] J. Beguinél, New Continuous Fiber Reinforced Thermoplastic Composites : An analysis of Interfacial Adhesion from the micro scale to the macro scale, in *Proceedings of the 20th International Conference on Composite Materials, Copenhagen, Denmark, July 19-24 (2015)*.
- [14] P.J. Herrera-Franco, L.T. Drzal, Comparison of methods for the measurement of fibre/matrix adhesion in composites, *Composites*, 23 (1992) 2-27.
- [15] B. Miller, P. Muri, L. Rebenfeld, A microbond method for determination of the shear strength of a fiber/resin interface, *Compos. Sci. Technol.*, 28 (1987) 17-32.
- [16] M.R. Piggott, Debonding and friction at fibre-polymer interfaces. I: Criteria for failure and sliding, *Compos. Sci. Technol.*, 30 (1987) 295-306.
- [17] J.T. Ash, W.M. Cross, D. Svalstad, J.J. Kellar, L. Kjerengtroen, Finite element evaluation of the microbond test: meniscus effect, interphase region, and vise angle, *Compos. Sci. Technol.*, 63 (2003) 641-651.
- [18] D. Tripathi, F.R. Jones, Single fibre fragmentation test for assessing adhesion in fibre reinforced composites, *J. Mater. Sci.*, 33 (1998) 1-16.

- [19] P. Zinck, H.D. Wagner, L. Salmon, J.F. Gerard, Are microcomposites realistic models of the fibre/matrix interface? Part I. Micromechanical modelling and Part II. Physico-chemical approach, *Polymer*, 42 (2001) 5401-5413 and 6641-6650.
- [20] C.C. Chamis, J.H. Sinclair, Ten-deg off-axis test for shear properties in fiber composites, *Exp.Mech.*, 17 (1977) 339-346.
- [21] A. Chapiro, Radical reactions in polymer gels and glasses, *Eur. Polym. J.*, 5 (1969) 43-54.
- [22] G. Odian, Radical Chain Polymerisation, in: *Principles of Polymerization*, Wiley, 4e edition, 2004, 198-350.
- [23] T. Benethuiliere, Physico-chemistry of vinylester/glass fiber interfaces used in SMC composites, in *Proceedings of the 20th International Conference on Composite Materials*, Copenhagen, Denmark, July 19-24 (2015).
- [24] E. Mäder, K. Grundke, H.J. Jacobasch, G. Wachinger, Surface, interphase and composite property relations in fiber-reinforced polymers, *Composites*, 25 (1994) 739-744.
- [25] K.A. Downes, J.L. Thomason, A method to measure the influence of humidity and temperature on the interfacial adhesion in polyamide composites, *Compos. Interfaces*, 22 (2015) 757-766.
- [26] L. Yang, J.L. Thomason, Development and application of micromechanical techniques for characterising interfacial shear strength in fibre-thermoplastic composites, *Polym. Test.*, 31 (2012) 895-903.
- [27] J.C. Halpin, J.L. Kardos, The Halpin-Tsai equations: a review, *Polym. Eng. Sci.*, 16 (1976) 344-352.
- [28] M.S. Madhukar, L.T. Drzal, Fiber-matrix adhesion and its effect on composite mechanical properties: I. Inplane and interlaminar shear behaviour of graphite/epoxy composites, *J. Compos. Mater.*, 25 (1991) 932-957.
- [29] F. Pierron, A. Vautrin, The 10° off-axis tensile test: A critical approach, *Compos. Sci. Technol.*, 56 (1996) 483-488.